Experimental Study and Analysis of a Full-Scale CFRP/CFCC Double-Tee Bridge Beam

Nabil F. Grace, Ph.D., P.E.
Professor and Chairman
Department of Civil Engineering
Lawrence Technological University
Southfield, Michigan

Tsuyoshi Enomoto
Engineer
Bridge and Structural Cable Department
Engineering Division
Tokyo Rope Mfg. Co., Ltd.
Tokyo, Japan

George Abdel-Sayed, Dr. Eng., P. Eng.
Professor Emeritus
Department of Civil Engineering
University of Windsor
Windsor, Ontario, Canada

Kensuke Yagi
Manager, Engineering
Construction Materials Division
Mitsubishi Chemical Functional
Products, Inc.
Tokyo, Japan

Loris Collavino, P.E.
President
Hollowcore Incorporated
Prestressed Systems, Inc.
Detroit, Michigan

This paper presents a study on the fabrication, instrumentation, and flexural testing of a full-scale double-tee (DT) beam, prestressed using bonded pretensioned CFRP Leadline™ tendons and unbonded carbon fiber composite cable (CFCC) post-tensioning strands. The beam was designed to simulate the performance of the DT beams used for the construction of the three-span Bridge Street Bridge, the first vehicular concrete bridge ever built in the United States that uses CFRP material as the principal structural reinforcement. Testing focused on measurement of strain distributions along the length and depth of the beam, transfer length, camber/deflection, cracking load, forces in post-tensioning strands, ultimate load-carrying capacity, and mode of failure. In addition, an analysis approach is presented to theoretically evaluate the response of the tested beam. It was observed that the ultimate failure of the beam was initiated by partial separation between the topping and the beam flange, which led to the crushing of the concrete topping followed by rupture of bottom tendons. The tested beam was found to have significant reserve strength beyond the service load. Theoretical calculations are similar in value to the corresponding experimental results – especially under the service load condition.

Concrete bridges prestressed and reinforced using carbon fiber reinforced polymer (CFRP) materials are being used worldwide.[1] However, the concrete bridges constructed using CFRP tendons are few in number.[1-7] The most recent example of this new technology is the Bridge Street Bridge,[8] the first CFRP prestressed concrete bridge built in the United States using CFRP Leadline™ tendons* and carbon fiber composite cable (CFCC) strands.†

Extensive research, funded by the National Science

Foundation, addressing the behavior of this new bridge system, was conducted on one-third scale bridge models in the Structural Testing Center at Lawrence Technological University (LTU) in Southfield, Michigan.[7,9-13] The results of this research formed the design basis that led to the double-tee (DT) beam tests and the award-winning Bridge Street Bridge design.

The objective of the full-scale testing presented here is to experimentally determine the various response parameters for the DT beam – a design almost identical to that used in the Bridge Street Bridge. The parameters include strains, deflections, forces in post-tensioning strands at service load, cracking load, and ultimate load conditions. Full-scale testing was required to verify the assumptions made in the analysis and design approach presented in Appendix A.

FABRICATION AND INSTRUMENTATION

The cross section of the DT test beam is shown in Fig. 1, while Fig. 2 shows the plan and elevation of the beam with the location of the externally draped CFCC post-tensioning strands. The concrete cross section consists of the DT precast section and 75 mm (3.0 in.) thick concrete topping. Total depth of the precast section is 1220 mm (48.0 in.) with a flange thickness of 150 mm (5.90 in.). Total width of flange is 2120 mm (83.5 in.).

Reinforcement consists of 10 rows of 10 mm (0.39 in.) diameter bonded prestressing CFRP Leadline™ tendons and 6 rows of 12.5 mm (0.5 in.) non-prestressing CFCC strands in each web of the DT beam. The vertical distance between adjacent rows of the prestressing tendons is 70 mm (2.8 in.). The cross section also consists of four externally draped 40 mm (1.57 in.) diameter post-tensioning CFCC strands and nineteen 10 mm (0.39 in.) diameter non-prestressing rods placed longitudinally in the flange.

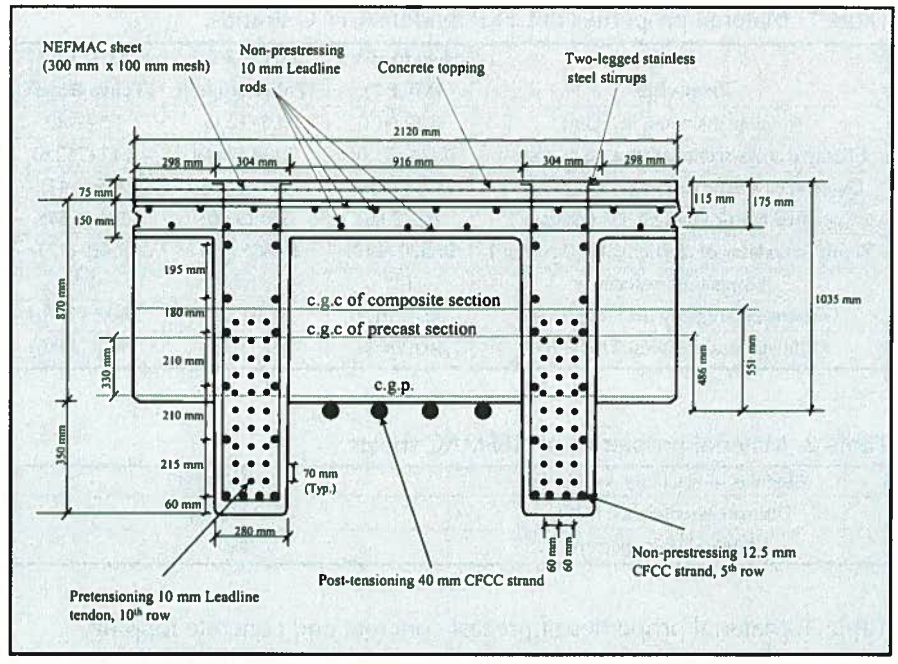

Fig. 1. Cross section of DT test beam at midspan.

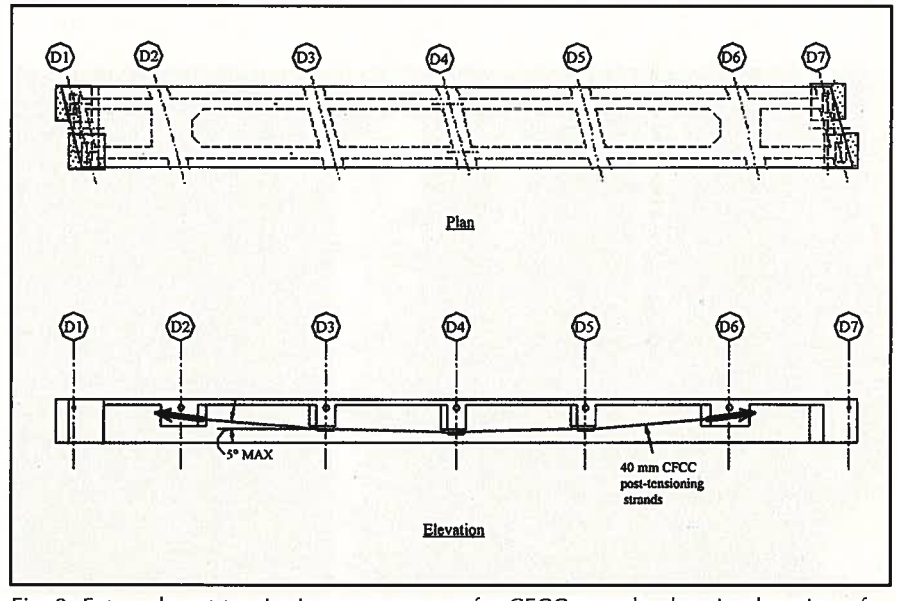

Fig. 2. External post-tensioning arrangement for CFCC strands, showing location of the seven diaphragms.

In addition, the flange is reinforced with two layers of transverse 10 mm (0.39 in.) diameter Leadline™ tendons. The post-tensioning strands are longitudinally draped between Diaphragms D2 and D6 and located at a depth of 1035 mm (40.8 in.) from the top surface of concrete topping at midspan. As shown in Fig. 2, the DT beam consists of seven diaphragms (D1 through D7). The total overall length of the DT beam is 20.88 m (68.5 ft), and the effective span is 20.40 mm (67.0 ft). The mechanical properties of the CFRP Leadline™ tendons and CFCC strands are given in Table 1, while the properties of the NEFMAC‡ reinforcing grid (used in the concrete topping) and the concrete are presented in Tables 2 and 3, respectively.

Fabrication

The DT test beam was cast using a single pan form incorporating the two stems, top flange, and seven transverse integral diaphragms. All fabrication activities took place at the precast

* Leadline™ tendons manufactured by Mitsubishi Chemical Functional Products, Inc., Japan.
† CFCC strands manufactured by Tokyo Rope Manufacturing Co., Ltd., Japan.
‡ NEFMAC grid reinforcement manufactured by Autocon Composites, Inc., Ontario, Canada.

Table 1. Material properties of CFRP tendons/CFCC strands.

Properties	Leadline™ (MCC[15])	CFCC 1 x 7 (Tokyo Rope[16])	CFCC 1 x 37 (Tokyo Rope[16])
Nominal diameter, in. (mm)	0.39 (10)	0.5 (12.5)	1.57 (40)
Effective cross-sectional area, sq in. (mm^2)	0.111 (71.6)	0.118 (76.0)	1.17 (752.6)
Guaranteed tensile strength, ksi (kN/mm^2)	328 (2.26)	271 (1.87)	205 (1.41)
Specified tensile strength, ksi (kN/mm^2)	415 (2.86)	305 (2.10)	271 (1.87)
Young's modulus of elasticity, ksi (kN/mm^2)	21,320 (147)	19,865 (137)	18,419 (127)
Elongation, percent	1.9	1.5	1.5
Guaranteed breaking load, kips (kN)	36.4 (162)	31.9 (142)	240.5 (1070)
Ultimate breaking load, kips (kN)	46 (204.7)	36 (160)	316.9 (1410)

Table 2. Material properties of NEFMAC sheets.

Modulus of elasticity, ksi (GPa)	12,540 (86.5)
Ultimate strength, ksi (MPa)	217 (1500)
Ultimate strain, percent	1.8

Table 3. Material properties of precast concrete and concrete topping.

Properties	Precast concrete	Concrete topping
Modulus of elasticity, ksi (GPa)	5320 (36.7)	4580 (31.6)
Strength, ksi (MPa)	7.81 (53.8)	5.7 (39.3)

Fig. 3. Pretensioned CFRP Leadline™ tendons at roller hold-down location.

plant, Prestressed Systems Inc., located in Windsor, Ontario, Canada.

The sequence of fabrication is given below:

1. Installation of the CFCC and CFRP mild reinforcement, steel stirrups, CFRP prestressing Leadline™ tendons, and other embedded items such as hold-up and hold-down devices, vibrating wire, and electrical resistance strain gauges in the formwork.

2. Installation and stressing of the pretensioned CFRP tendons.

3. Casting and curing of concrete.

4. Release of pretensioned CFRP Leadline™ tendons after concrete achieved desired strength.

5. Removal of the prestressed beam from the form.

6. Installation of the longitudinal CFCC post-tensioning strands and applying 60 percent of the total post-tensioning force.

Except for those in Row 10, all Leadline™ tendons were draped prior to pretensioning using hold-down and hold-up roller devices. These tendon-holding rollers were specially fabricated using soft materials. All Leadline™ tendons were pretensioned using series of conventional steel strands, CFRP-tendon anchor systems, couplers, steel strand anchor chucks, and a hydraulic jack. Fig. 3 shows the pretensioned CFRP Leadline™ tendons at a roller hold-down point.

When the concrete achieved adequate strength – 45.9 MPa (6.66 ksi) in 48 hours – CFRP Leadline™ tendons were released in the sequence shown in Fig. 4. A typical draped tendon with hold-up and hold-down arrangements is also illustrated in Fig. 4. A close-up view of pretensioned tendons, CFCC non-prestressing strands, and flange reinforcement is provided in Fig. 5.

Four externally draped post-tensioning CFCC strands were installed after the release of the pretensioning tendons and form removal. Fig. 6 reveals the post-tensioning strands as seen from below the beam. Post-tensioning anchorage details at Diaphragm D6 are represented in Fig. 7. Each post-tensioning strand was tensioned using a special apparatus (see Fig. 8) using specific sequencing.

A special bearing system at Diaphragms D3, D4, and D5 was designed and constructed to allow the design (anticipated) movement of the external CFCC strands due to traffic loads and temperature changes, and to accommodate construction tolerances (see Fig. 6). This bearing system was critical to provide an almost friction-less bearing surface between the CFCC strands and the diaphragm concrete.

Instrumentation

The instrumentation installed in the test beam was selected to achieve a set of measurement objectives. These measurements included the following:

- Pretensioned load applied to CFRP Leadline™ tendons.
- Transfer length of pretensioned CFRP Leadline™ tendons after release.
- Beam camber/deflections during fabrication/construction sequence.
- Concrete strain distributions in beam cross section and concrete topping.
- Forces in CFCC post-tensioning strands.

Measurement of Pretensioning Forces

Pretensioning forces were measured using a load cell installed between the stressing jack at the live end and the chuck anchor, and these forces were recorded on a read-out device. A few load cells were also positioned at the dead end of selected tendon lines between the steel strand anchor chuck and the bulkhead for spot checking and verification of the readings taken at the live end.

In addition to these load cells, the elongation of the tendons and gauge pressure of the hydraulic pump were used to verify the desired pretensioning forces. Once the jacking force, gauge pressure, and elongation had been recorded, the stressing assembly was transferred to the next tendon; this procedure was continued until all 60 Leadline™ tendons were stressed.

The total prestressing forces in each CFRP tendon in Rows 1 through 5 and Rows 6 through 10 were 82.3 and 86.7 kN (18.5 and 19.5 kips), respectively, after seating losses, or about 40 and 42 percent of the ultimate breaking load of the Leadline™ tendons, respectively. Load cells located at the dead end were continuously monitored during and after placement of the concrete to measure any changes in the pretensioning forces during concrete placing and curing.

Measurement of Transfer Length

Transfer length of the pretensioning tendons was measured using seven vibrating wire strain gauges with an effective gauge length of 152 mm (6.0 in.). Gauges were installed along one web at both ends of the beam during fabrication. Strain gauges were installed end to end beginning at the end of the beam and extending over a distance of approximately 1065 mm (42.0 in.). All seven gauges at each beam end were located at an elevation coinciding with the centroid of the total designed pretensioning force, and staggered about the mid-width centerline of the web.

Measurement of Early Age Camber

A complete history of early age deflection in the test beam was obtained

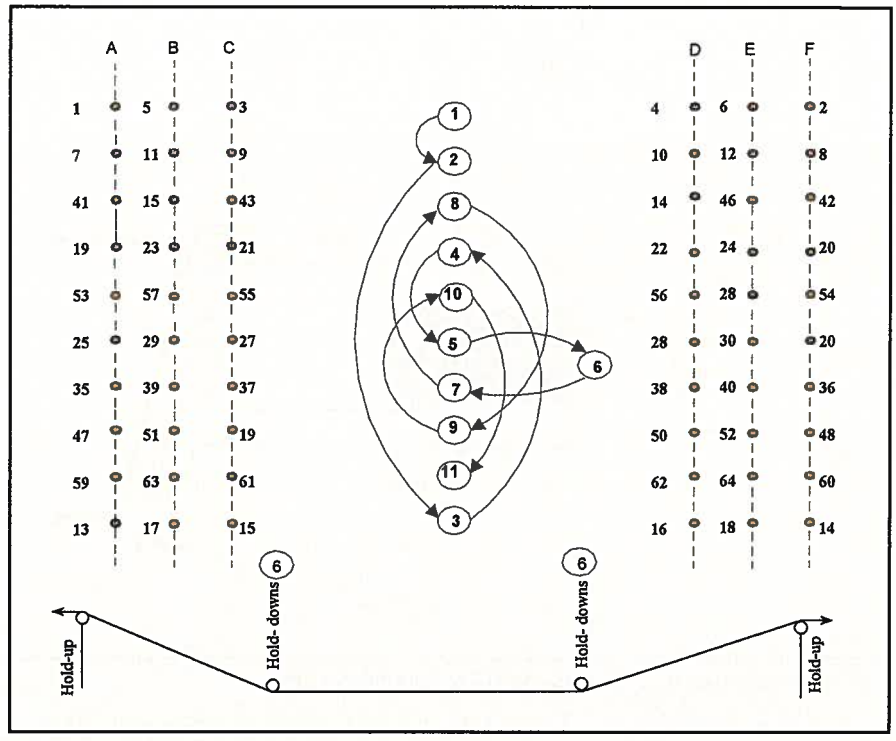

Fig. 4. Release pattern for 60 pretensioned tendons.

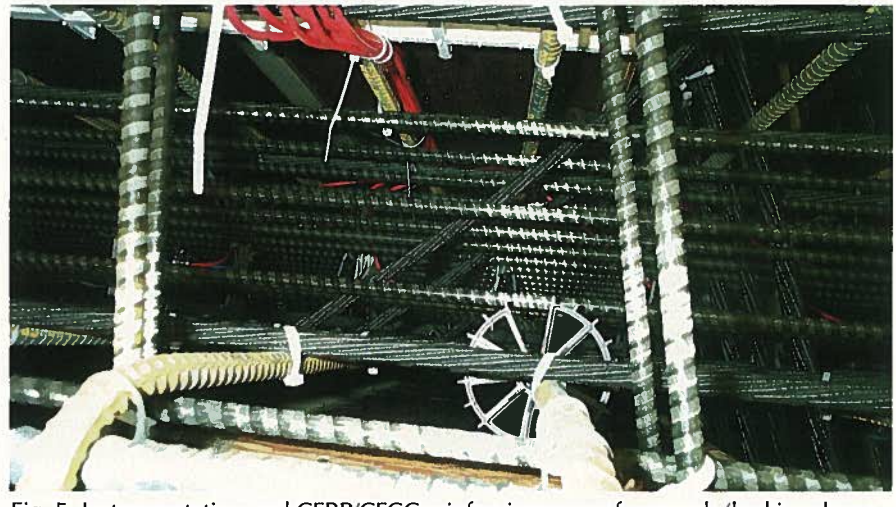

Fig. 5. Instrumentation and CFRP/CFCC reinforcing cage of one web (looking down from top).

Fig. 6. Externally draped post-tensioning CFCC strands (looking from below DT beam).

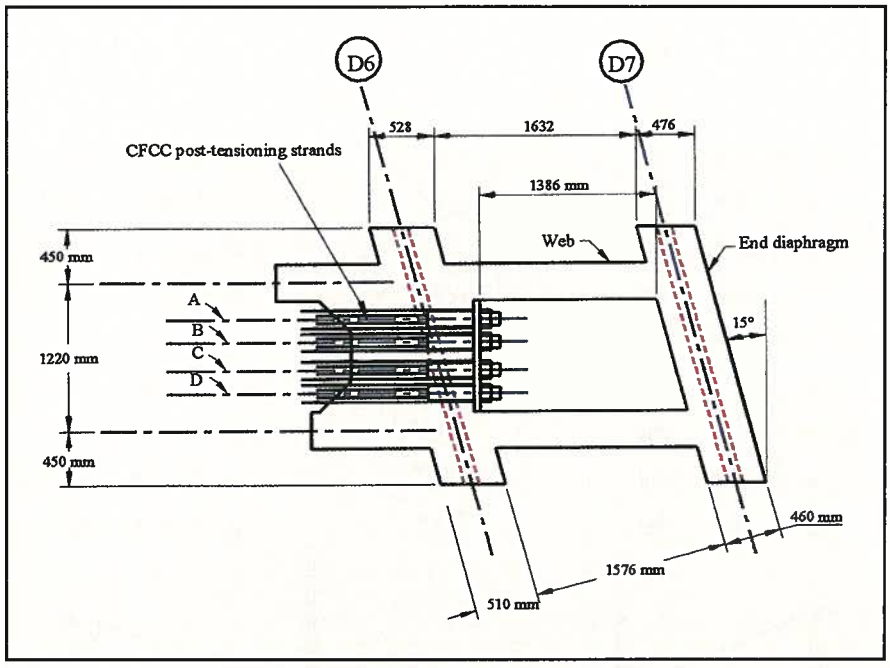

Fig. 7. Post-tensioning anchorage details at Diaphragm D6.

Fig. 8. Post-tensioning apparatus for a CFCC externally draped strand.

Fig. 9. NEFMAC reinforcing grid placed over the flange top.

using elevation reference points embedded in the concrete surface. Elevation points were located along the top flange of the test beam at midspan, at two quarter-span points, and near the beam ends. Prior to prestressing tendon release, elevation measurements were recorded for each point and used as a reference for all subsequent measurements. After tendon release, measured changes in elevation relative to the initial pre-release values were used to calculate beam camber due to prestressing at the mid- and quarter-span points.

Total camber due to pretensioning force and initial post-tensioning force was 20.1 mm (0.79 in.). Net camber after the addition of the topping and the final stage of post-tensioning was 14.3 mm (0.56 in.). Note that a total loss of 6.4 mm (0.25 in.) of midspan camber occurred due to changes in the support location and transportation of the beam from the fabrication plant to the testing facility.

The elevation of each reference point was determined using a precision level and surveying rod with a high-resolution scale. The precision level used for this application required an internal micrometer capable of resolving elevation readings to the nearest 0.030 mm (0.001 in.). The top surface of each embedded reference point incorporated a machined indentation to match the pointed end of the surveyor's rod.

Measurement of Concrete Strains

Embedded electrical-resistance strain gauges were installed for measuring strain distributions along the depth of cross sections at midspan and quarter-spans. A total of 30 strain gauges were installed in the test beam. Of these 30 gauges, 21 were installed in the precast section at the fabrication plant, while the remaining nine gauges were installed in the cast-in-place concrete topping at the testing facility.

Measurement of Post-tensioning Forces

Prior to post-tensioning, all four post-tensioning strands were instrumented with load cells at one end (see Fig. 8). The load cells were installed

between the lock nut on the strand anchor/head and the bearing plate embedded in the transverse Diaphragm D2 near the end of the beam (see Fig. 2).

Post-tensioning was applied to the four CFCC strands in two separate stages (initial and final). The initial post-tensioning (at the precast yard in Windsor, Canada) consisted of applying 60 percent of the total desired post-tensioning force [449 kN (101 kips)], equal to 32 percent of the ultimate breaking load of CFCC post-tensioning strands on the precast DT beam. Final post-tensioning was applied at the Construction Technology Laboratories, Inc. (CTL), testing facility in Skokie, Illinois, after casting the concrete topping. Final post-tensioning consisted of the remaining 40 percent of the total post-tensioning force.

Each stage of post-tensioning was applied in two parts. During the first part, approximately 50 percent [133.5 kN (30.0 kips)] of the required force was applied by pulling the strands from one end as shown in Fig. 8. After completion of the first part, the post-tensioning setup was moved to the opposite end where the remaining 50 percent of the required force was applied.

At the precast facility, the initial post-tensioning was applied with the beam supported at Diaphragms D2 and D6 at intermediate transverse locations. The beam remained supported in this manner until delivered to the CTL test facility. The beam support configuration prevented the development of additional tensile strain due to dead loads.

At CTL, final post-tensioning was applied with the beam supported at the End Diaphragms D1 and D7 after the placement of the concrete topping to simulate the post-tensioning of the actual DT beams used in the Bridge Street Bridge. The average measured strand force after the initial post-tensioning was 268 kN (60.3 kips), while the average measured strand force immediately after the final post-tensioning was 449 kN (101 kips).

CTL followed stressing procedures similar to those of the precast plant: the remaining 40 percent of the total post-tensioning force was applied prior to the onset of structural testing

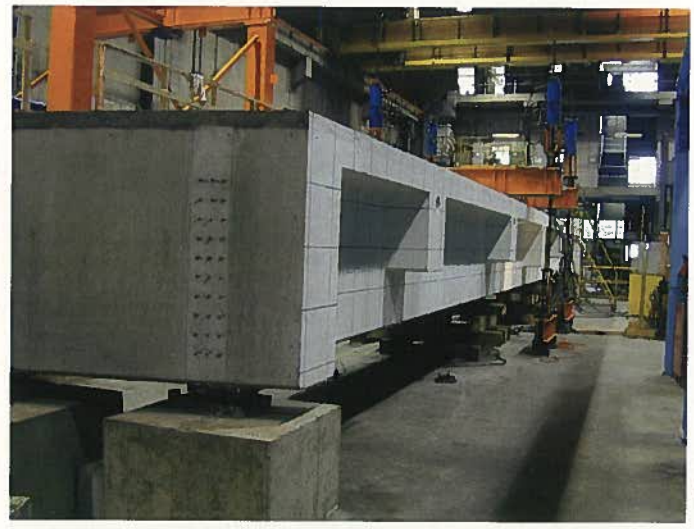

(a) Test setup for flexural loading.

(b) Support condition of test beam.

Fig. 10. Flexural load testing at the CTL testing facility.

(described below). The average measured force in the CFCC strand prior to the test was 443 kN (99.6 kips), which was slightly less than that observed immediately after the final post-tensioning.

Casting of Concrete Topping

Finally, a 75 mm (3.0 in.) thick concrete topping was cast over the top flange of the precast DT beam. In preparation for casting, a CFRP NEFMAC grid reinforcement (see Fig. 9) was installed over the top flange of the beam. In addition, the nine remaining embedded concrete strain gauges required for concrete strain distribution measurements were installed at midspan and the two quarter-span locations.

The NEFMAC reinforcement was supplied in the form of grid sheets, each with a transverse dimension of 2083 mm (82.0 in.). Each grid sheet incorporated longitudinal reinforcement elements spaced at 300 mm (12 in.) and transverse elements spaced at 100 mm (4 in.) intervals. The NEFMAC reinforcement was supported on 25 mm (1.0 in.) high plastic slab bolsters; these were epoxy-anchored to the top surface of the beam flange. Each grid sheet was secured to the slab bolster using plastic ties.

TEST SETUP

The flexural loading test setup and support condition for the beam are shown in Figs. 10a and 10b, respectively. The beam was loaded along two lines to create a 3658 mm (12.0 ft) wide constant moment region sym-

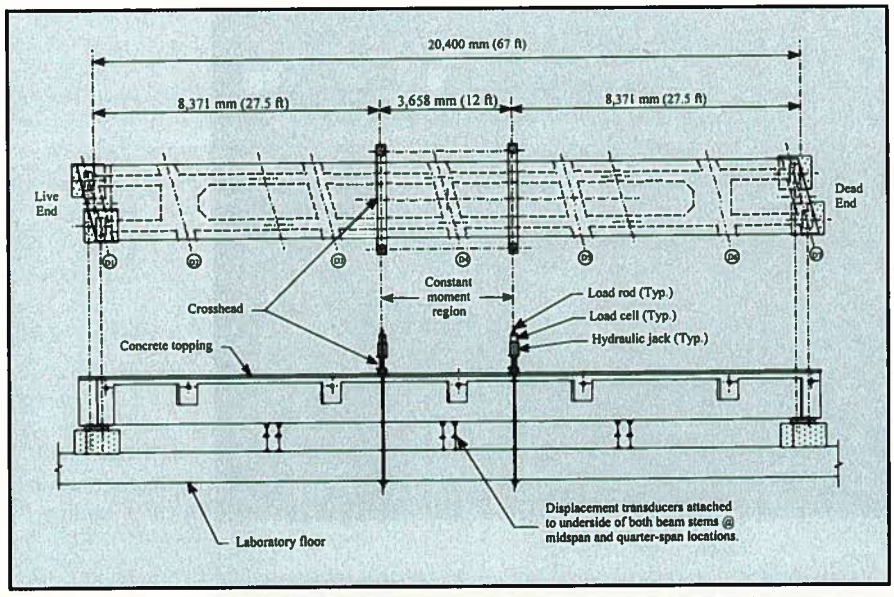

Fig. 11. Location of four-point loading system, showing location of displacement transducers.

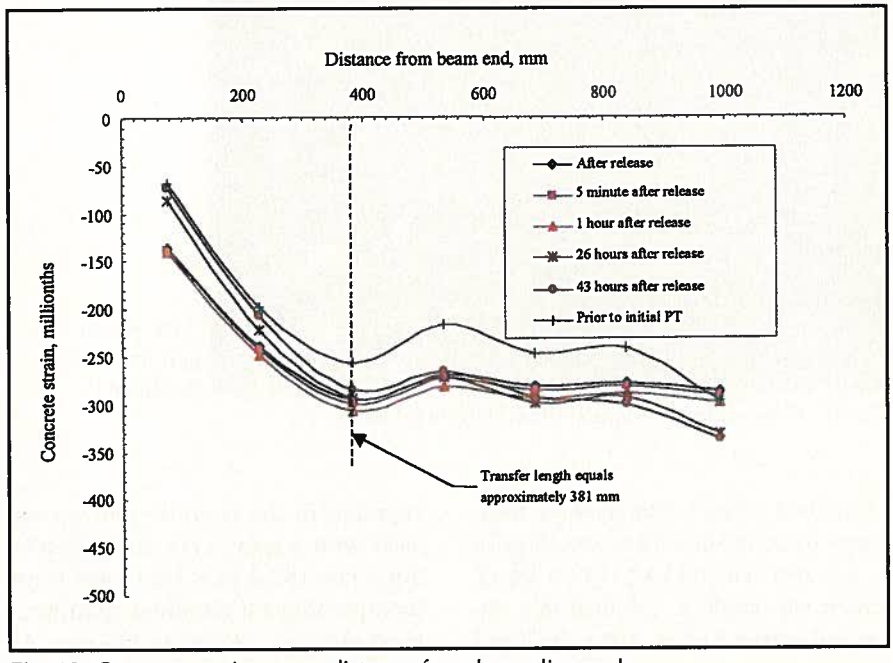

Fig. 12. Concrete strain versus distance from beam live end.

metrical about midspan (see Fig. 11). The loading lines were oriented orthogonally to the longitudinal centerline of the beam. Along each line, load was applied at two bearing points that were coincident with the beam webs. Roller supports in Fig. 10b were used at each beam end to allow both longitudinal movement and rotation under the load.

Load was applied using a series of hydraulic jacks with load and extension capability sufficient to induce flexural failure. All loads applied to the beam during the test were monitored using load cells. Beam displacements at mid- and quarter-span locations were monitored using two displacement transducers at each location attached to the underside of the two webs.

In addition to the applied loads and deflections, output from the concrete strain gauges installed for measuring strain distribution at midspan and two quarter-span sections – and from the longitudinal CFCC strand load cells – was monitored during the flexural test. Output data from instrumentation were monitored throughout the test and recorded at each loading increment.

RESULTS AND DISCUSSION

Transfer Length

Fig. 12 shows the concrete strain plotted against distance from the live end of the beam. The strain values refer to data recorded at various time intervals (immediately, 5 minutes, 1 hour, 26 hours, and 43 hours after release, and prior to initial post-tensioning). It can be seen from Fig. 12 that the transfer length (the distance from the beam end at which full effective prestress is transferred to the concrete) is approximately 381 mm (15.0 in.), compared to a theoretical value of 419 mm (16.5 in.) [based on Eq. (4) in Reference 11].

Thus, experimental and calculated results for transfer length of Leadline™ tendons are similar in value. As indicated by the measured data, concrete strains gradually increased with distance from the beam end until strains stabilized or became uniform (at the location of the third vibrating-wire strain gauge).

Strain Distribution after Post-tensioning and Service Load

The distribution of concrete strains along the depth of the cross sections [at mid- and two quarter-span (Q-S) locations] after the final post-tensioning and due to service load is shown in Figs. 13a and 13b, respectively. Fig. 13a indicates that after final post-tensioning, the strain at the top surface of the concrete topping (at midspan) is small and tensile in nature, whereas the strain throughout the depth of cross section is in the compression range.

High compressive strain developed at the bottom at each cross section location. The developed compressive strain levels were desirable to eliminate any potential cracking problems under service load/traffic condition. The DT cross section dimensions, the placement and arrangement of prestressing tendons, as well as post-ten-

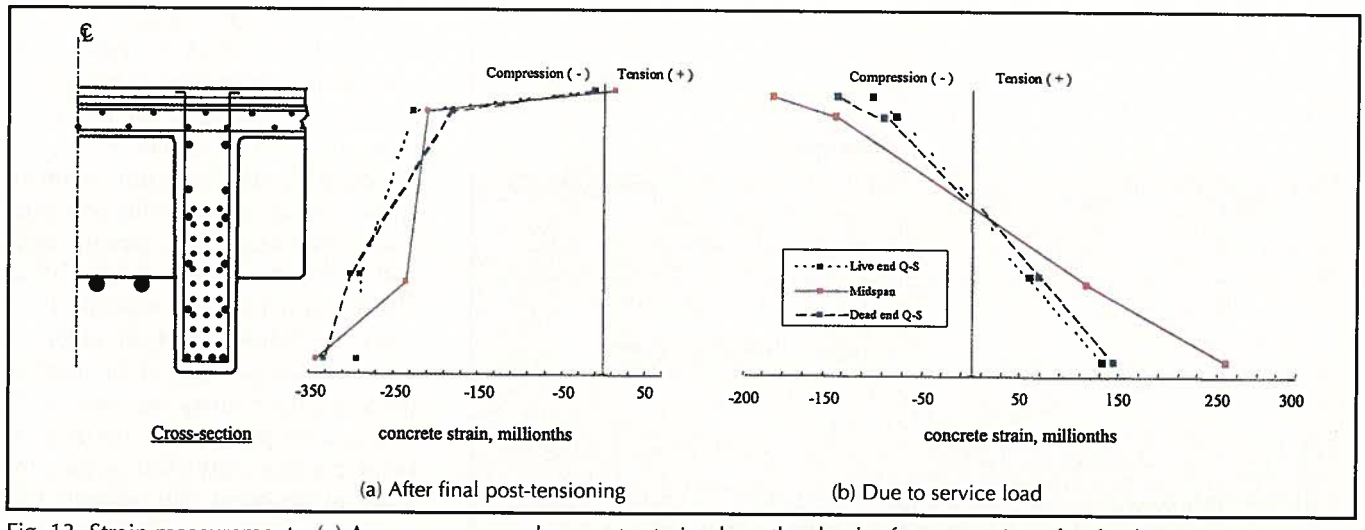

Fig. 13. Strain measurements: (a) Average measured concrete strain along the depth of cross section after final post-tensioning; and (b) Strain due to service load.

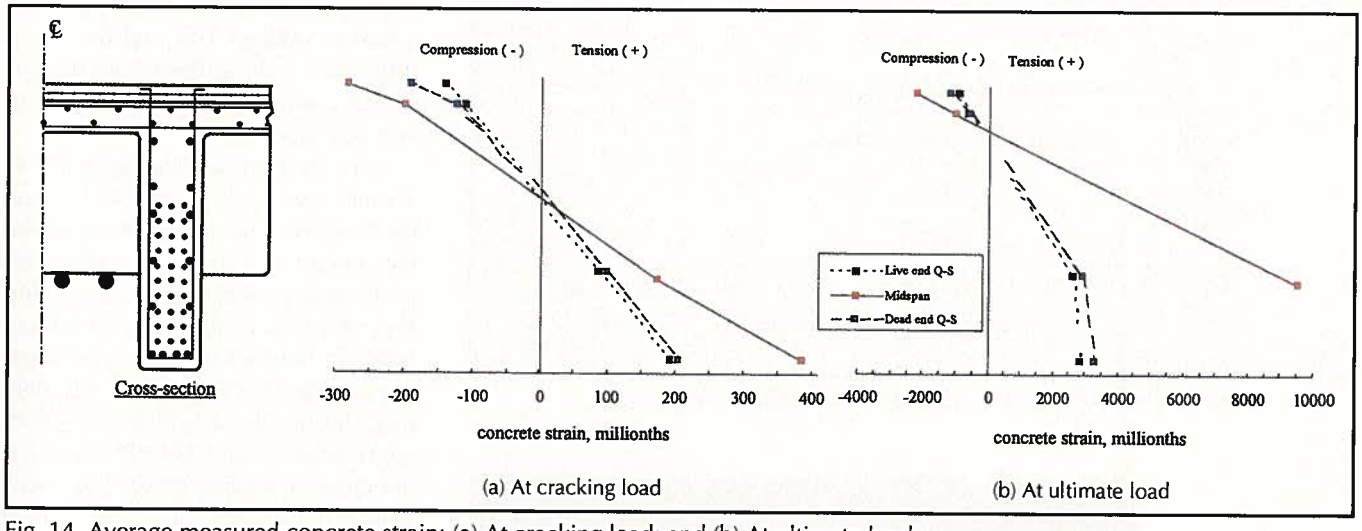

Fig. 14. Average measured concrete strain: (a) At cracking load; and (b) At ultimate load.

sioning strands, were selected so that no cracking would occur under service loads.

Superposition of the concrete strain readings due to pretensioning and post-tensioning shown in Fig. 13a and the service load condition in Fig. 13b indicates that the net strain at the bottom and top surfaces of the beam is compressive. This strain result is desirable in eliminating any potential cracking problems in the CFRP prestressed concrete beam under service loading.

Strain Distribution at Cracking and Ultimate Loads

After reaching the service load level, incremental loading of the DT beam continued to reach the applied load corresponding to the development of the first concrete crack. To accomplish this objective, the beam was loaded in suitably small increments so that careful observations could be made of the bottom surface for beam strains within the constant moment region. After application of each increment, loading was suspended to allow sufficient time to visually inspect for cracking.

The total applied load corresponding to the development of the first crack was found to be 643.9 kN (144.7 kips). Figs. 14a and 14b show the concrete strain distributions along the depth of cross sections at mid- and quarter-span (Q-S) locations at the cracking and ultimate load conditions. Note that the strain readings shown in Fig. 14 are only due to the applied loads and do not include the pretensioning and post-tensioning effects.

Fig. 14 shows that the strain distributions at the quarter-span sections are very close in value. In Fig. 14b, the ultimate strain at the top of concrete topping has reached a compressive strain as high as 0.0025, whereas the webs are in tension. Note that data for web strain at the midspan section under the ultimate load condition in Fig. 14b are not presented due to failure of the corresponding strain gauge.

Superposition of the concrete strain readings due to pretensioning and post-tensioning and the cracking load conditions shown in Figs. 13a and 14a indicates that the net strain at the bottom of the beam is close to the strain value corresponding to the modulus of rupture of concrete.

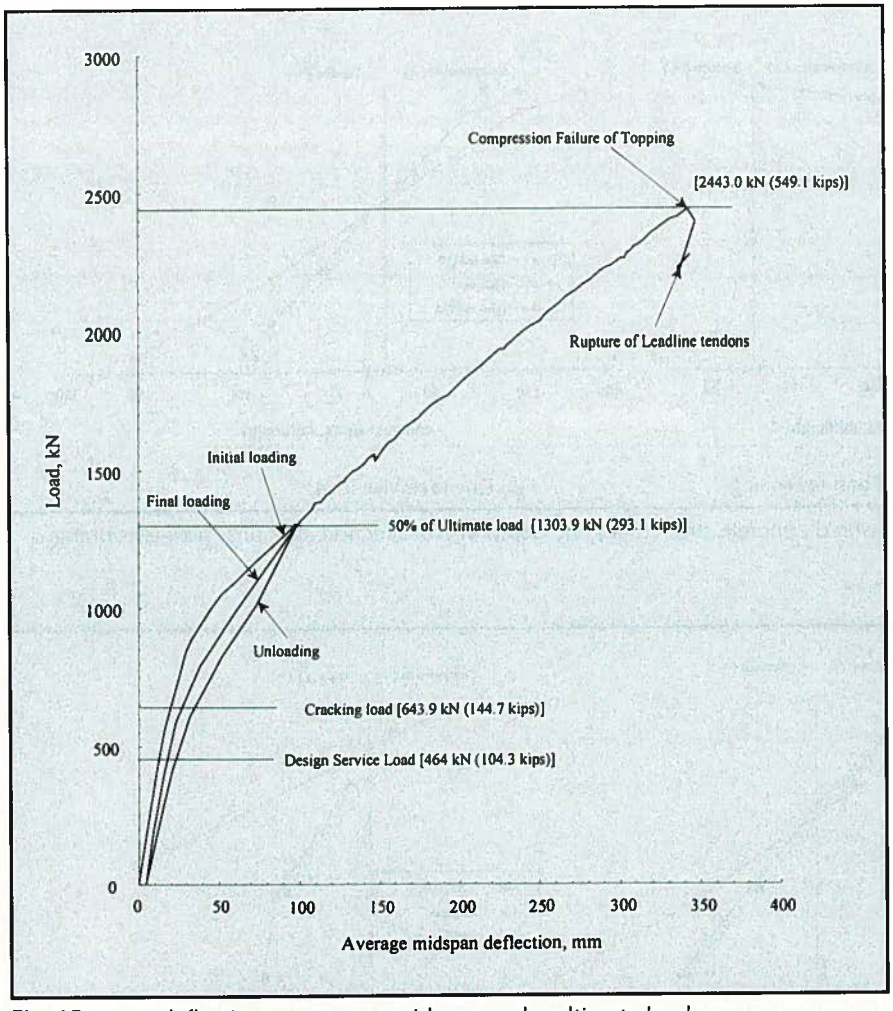

Fig. 15. Beam deflection response at midspan under ultimate load.

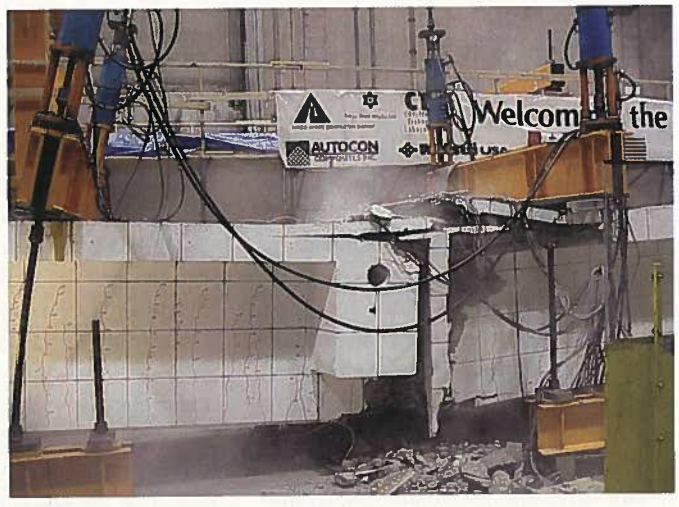

Fig. 16. Closeup of beam failure. External unbonded CFCC post-tensioning strands did not rupture.

ULTIMATE BEHAVIOR OF DT BEAM

Ultimate flexural strength was reached when the beam was incrementally loaded to a total load of 1303.9 kN (293.1 kips) and then unloaded (see Fig. 15). This load represents about 50 percent of the actual ultimate strength. The loading and unloading sequence was necessary to evaluate the ductility of the beam. After the initial loading and unloading sequence, the beam was incrementally loaded to induce flexural failure.

The ultimate load applied during the test was 2443.0 kN (549.1 kips). Average midspan deflections at the service, cracking, and ultimate load conditions were 12.82, 18.67, and 342.3 mm (0.505, 0.74, and 13.48 in.), while the corresponding forces in the unbonded post-tensioning CFCC strands were 450.0, 453.8, and 807.1 kN (101.1, 102.0, and 181.4 kips), respectively.

Fig. 16 indicates that the failure of the DT beam occurred in the constant moment region along one side of the midspan Diaphragm D4 and that the failure plane extended across the width of the beam. The ultimate failure of the DT beam was initiated by partial separation between the bottom of the topping and top of the beam flange, which led to crushing of the concrete topping. This was due to the difference in the stiffness and strength of the concrete topping and precast concrete section.

After the concrete topping failed, an attempt was made to further increase the load. As Fig. 15 shows, however, the rupture of Leadline™ tendons led to the beam collapse without any further increase in the load. The force levels in the four CFCC post-tensioning strands (see Fig. 17) nearly doubled during the test, increasing from approximately 443 kN (99.6 kips) at the onset of loading to 807 kN (181.4 kips) at the ultimate load, yet none of the CFCC strands nor their anchors ruptured.

ANALYSIS

An analysis of experimental results obtained from the full-scale DT test beam is presented in this paper. A theoretical analysis was also developed to predict the strength and failure mode of the DT test beam. The strains, stresses, and forces in strands, and deflection of the beam were calculated for the service and ultimate loading conditions.[14] Details of the theoretical analysis and calculations are presented in Appendix A.[15-20]

CONCLUSIONS

Based on the results of the test program, the following conclusions can be drawn:

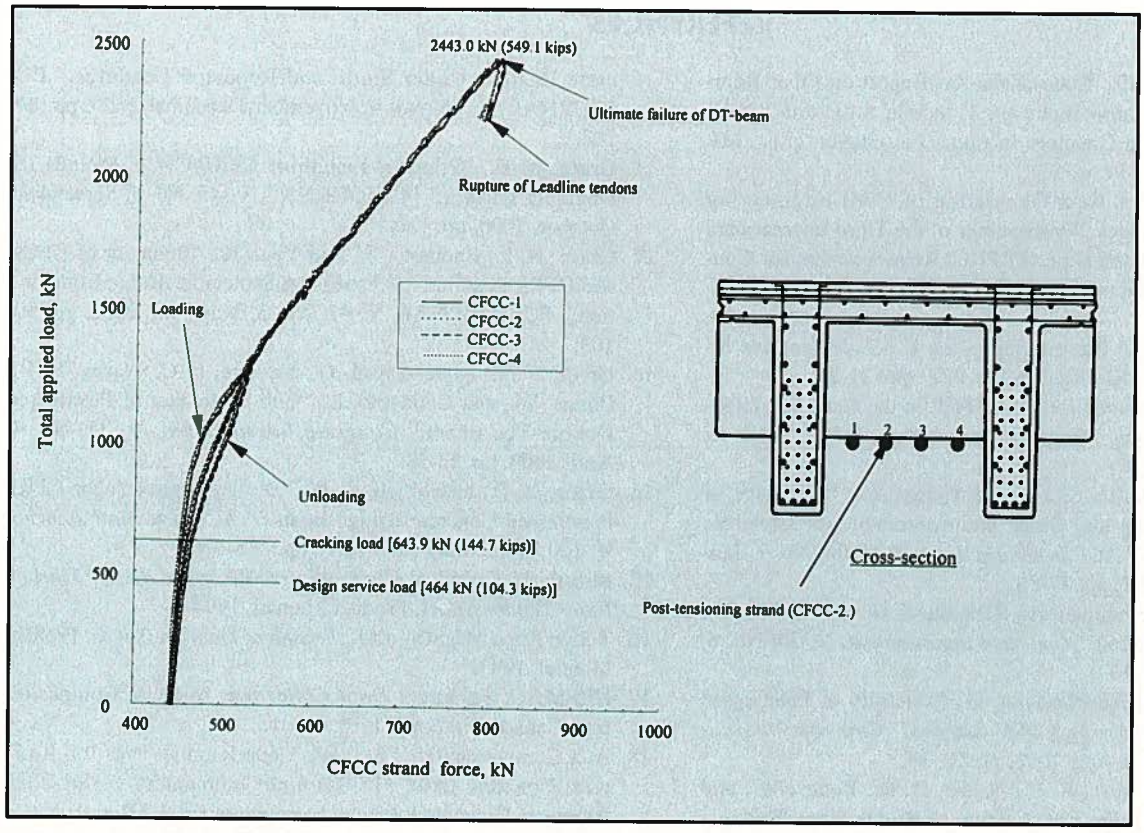

Fig. 17. Force in CFCC post-tensioning strands, indicating response under ultimate load and failure of DT beam.

1. The test results and construction experience gained from this evaluation have been implemented in the design documents for the 12 DT beams required for the construction of the Bridge Street Bridge.

2. The DT beam had significant reserve strength beyond the service load. The ultimate load and the cracking load of the DT beam were, respectively, approximately 5.3 and 1.4 times the service load.

3. The combined internal and external prestressing forces induced the designed compressive strain in the cross section.

4. The ultimate failure of the DT beam was initiated by partial separation between the topping and the beam flange, which led to crushing of the concrete topping followed by rupture of the internal prestressing tendons.

5. Significant cracking was observed prior to failure. However, none of the external unbonded CFCC post-tensioning strands nor their anchors ruptured.

6. Theoretical values and experimental results are very close, especially under service load condition. The theoretical nominal moment capacity of the DT beam is about 0.9 percent lower than the corresponding experimental value, whereas the predicted forces in the unbonded post-tensioning strands at the service and ultimate load conditions are 0.5 and 6.1 percent lower than corresponding experimental values.

ACKNOWLEDGMENTS

The DT beam for this study was constructed by Prestressed Systems Inc. (PSI), Windsor, Ontario, Canada, and tested by Construction Technology Laboratories, Inc. (CTL), Skokie, Illinois. Hubbell, Roth & Clark (HRC), Consulting Engineers, Bloomfield Hills, Michigan, provided the entire design, drawing details, and construction administration services. The City of Southfield and the Federal Highway Administration jointly funded the instrumentation and testing of the DT beam.

The National Science Foundation, Division of Civil and Mechanical Systems, funded the research activities, testing of several one-third-scale models (conducted in the Structural Testing Center at Lawrence Technological University), and the analytical evaluation of the full-scale testing.

Mitsubishi Chemical Functional Products, Inc., Tokyo Rope Manufacturing Co. Ltd., Autocon Composites Inc., Toronto, Canada, Sumitomo Corporation of America, and Mitsui USA Corporation also supported the ongoing research investigation. The tireless efforts of Drs. S. B. Singh and T. P. Murphy in these research and testing investigations are highly appreciated.

The authors also appreciate the technical comments of Dr. G. Tadros and the many constructive comments of the PCI JOURNAL reviewers.

REFERENCES

1. ACI Committee 440, "State-of-the-Art Report on Fiber Reinforced Plastic Reinforcement for Concrete Structures," ACI 440R-96, American Concrete Institute, Farmington Hills, MI, 1996, 153 pp.
2. Rizkalla, S. H., "A New Generation of Civil Engineering Structures and Bridges," Proceedings of the Third International Symposium on Nonmetallic (FRPRC) Reinforcement for Concrete Structures, Sapporo, Japan, V. 1, October 1997, pp. 113-128.
3. Dolan, C. W., "FRP Prestressing in the U.S.A.," *Concrete International*, V. 21, No. 10, October 1999, pp. 21-24.
4. Tadros, G., "Provisions for Using FRP in the Canadian Highway Bridge Design," *Concrete International*, V. 22, No. 7, July 2000, pp. 42-47.
5. Fam, A. Z., Rizkalla, S. H., and Tadros, G., "Behavior of CFRP Prestressing and Shear Reinforcements of Concrete Highway Bridges," *ACI Structural Journal*, V. 94, No. 1, January-February 1997, pp. 77-86.
6. Shehata, E., Abdelrahman, A., Rizkalla, S. H., and Tadros, G., "The New Generation," *Concrete International*, V. 20, No. 6, June 1998, pp. 35-38.
7. Grace, N. F., and Abdel-Sayed, G., "Ductility of Prestressed Concrete Bridges Using CFRP Strands," *Concrete International*, V. 20, No. 6, June 1998, pp. 25-30.
8. Grace, N. F., Navarre, F. C., Nacey, R. B., Bonus, W., and Collavino, L., "Design-Construction of Bridge Street Bridge – First CFRP Bridge in the United States," PCI JOURNAL, V. 47, No. 5, September-October 2002, pp. 20-35.
9. Grace, N. F., and Abdel-Sayed, G., "Behavior of Externally Draped CFRP Tendons in Prestressed Concrete Bridges," PCI JOURNAL, V. 43, No. 5, September-October 1998, pp. 88-101.
10. Grace, N. F., "Response of Continuous CFRP Prestressed Concrete Bridges Under Static and Repeated Loadings," PCI JOURNAL, V. 45, No. 6, November-December 2000, pp. 84-102.
11. Grace, N. F., "Transfer Length of CFRP/CFCC Strands for Double-T Girders," PCI JOURNAL, V. 45, No. 5, September-October, 2000, pp. 110-126.
12. Grace, N. F., Enomoto, T., and Yagi, K., "Behavior of CFCC and CFRP Leadline™ Prestressing System in Bridge Construction," PCI JOURNAL, V. 47, No. 3, May-June 2002, pp. 90-103.
13. Grace, N. F., Abdel-Sayed, G., Navarre, F. C., Nacey, R. B., Bonus, W., and Collavino, L., "Full-Scale Test of Prestressed Double-Tee Beam," *Concrete International*, V. 25, No. 4, April 2003, pp. 52-58.
14. Grace, N. F., and Singh, S. B., "Design Approach for CFRP Prestressed Concrete Bridge Beams," *ACI Structural Journal*, V. 100, No. 3, May-June 2003, pp. 365-376.
15. Mitsubishi Chemical Corporation (MCC), *Leadline™ Carbon Fiber Tendons/Bars*, Product Manual, 1994.
16. Tokyo Rope Mfg. Co. Ltd., *Technical Data on CFCC*, Product Manual, 1993.
17. NEFMAC, *Technical Data Collection*, Autocon Composites Inc., Canada, 1996, pp. 1-10.
18. ACI Committee 318, "Building Code Requirements for Structural Concrete (ACI 318-02) and Commentary (318R-02)," American Concrete Institute, Farmington Hills, MI, p. 105.
19. Chad, R. B., and Dolan, C. W., "Flexural Design of Prestressed Concrete Beams Using FRP Tendons," PCI JOURNAL, V. 46, No. 2, March-April 2001, pp. 76-87.
20. Naaman, A. E., and Alkhairi, F. M., "Stress at Ultimate in Unbonded Post-tensioning Tendons: Part 2 – Proposed Methodology," *ACI Structural Journal*, V. 88, No. 6, November-December 1991, pp. 683-692.

APPENDIX A – ANALYSIS PROCEDURE

The following procedure illustrates the steps for predicting the behavior of the full-scale pretensioned and post-tensioned DT test beam. The material properties of the tendons, strands, NEFMAC grids, and concrete are presented in Table 1. It should be noted that the term "tendon" is used for Leadline™ rods and "strand" is used for CFCC cables throughout the paper. It should also be noted that the cross-sectional area of NEFMAC grids has not been included in the analysis presented below:

Step 1 — Calculate required moment capacity:

Total dead load of beam = 142 kips
Dead load /unit length, W_d = 142/67 = 2.12 kip/ft
Dead load moment at midspan:

$$M_D = \frac{W_d L^2}{8}$$
$$= \frac{2.12 \times 67^2}{8}$$
$$= 1188.8 \text{ kip-ft}$$

Let W be the total midspan load applied through 4-point loading system. The distance between the center of each support to the nearest load point = 27.5 ft
Design service live load = 104.3 kips
Service live load moment at midspan,

$$M_L = \frac{104.3 \times 27.5}{2}$$
$$= 1434.13 \text{ kip-ft}$$

Required moment capacity of the section,

$$M_{required} = 1.4M_D + 1.7M_L \quad \text{(ACI 318-02)}$$
$$= 4102.34 \text{ kip-ft}$$

Step 2 — Calculate balanced ratio, ρ_b:

$$\rho_b = 0.85\beta_1 \frac{f'_c}{f_{fu}} \frac{\varepsilon_{cu}}{\varepsilon_{cu} + \varepsilon_{fu} - \varepsilon_{pbmi}} \quad \text{(A1)}$$

where

f'_c = strength of precast concrete = 7.81 ksi (see Table 3)
ε_{fu} = specified ultimate strain of bonded pretensioning tendons = 0.019 (see Table 1)
f_{fu} = specified strength of bonded pretensioning tendons = 415 ksi (see Table 1)
β_1 = 0.85 – [(7810 – 4000)/1000] × 0.05 = 0.66 (ACI 318-02)

Based on experimental results, 25 percent loss in the prestressing force in the bonded tendons is considered. The initial effective strain in bottom pretensioning tendons, ε_{pbmi}, can be calculated as follows:

$$\varepsilon_{pbmi} = \frac{19.5 \times 0.75}{0.111 \times 21{,}320}$$
$$= 0.0062$$

Based on experimental observation, the ultimate strain in concrete, ε_{cu}, is taken as 0.0025. This value of strain is very close to the value of 0.003 recommended by ACI 318-02. The use of measured value of crushing strain in theoretical evaluation will amount to an accurate comparison of the theoretical and experimental values of the ultimate load carrying capacity of the DT beam. Substituting the values in Eq. (A1) yields ρ_b = 0.0017.

Step 3 — Calculate cracking moment, M_{cr} and cracking load, P_{cr}:

Modulus of rupture of concrete,
$f_r = 6.0\sqrt{f'_c}$
= 530 psi
Various sectional properties of the DT beam section (see Fig. A1) are presented in Table A1.
Total effective pretensioning force,
$F_{pre} = 1139.3 \times 0.75$
= 854.5 kips
Total effective post-tensioning force, F_{post} = 397.8 kips
Stress at the bottom fiber of the section due to pretensioning force,

$$(\sigma_c)_{b1} = -\frac{F_{pre}}{A_p} - \frac{F_{pre}\, e_b}{S_{bp}} \quad \text{(A2)}$$

Here, A_p and S_{bp} are cross-sectional area and section modulus (with respect to bottom fiber) of precast section, respectively; e_b is the eccentricity of resultant pretensioning force with respect to the centroid of the precast section. From Table A1, A_p = 1462 sq in., S_{bp} =11,192 in.^{3}, and e_b = 13 in. Substituting values in Eq. (A2) results in $(\sigma_c)_{b1}$ = –1.577 ksi.

Since 60 percent of the total post-tensioning force was used to prestress the precast DT concrete section and the remaining 40 percent of the total post-tensioning force was applied on the composite concrete section (DT beam plus concrete topping), then the stress at the bottom fiber of section due to post-tensioning force, $(\sigma_c)_{b2}$, is:

$$(\sigma_c)_{b2} = -\frac{0.6 \times F_{post}}{A_p} - \frac{0.6 \times F_{post} e_{up}}{S_{bp}} - \frac{0.4 \times F_{post}}{A_c} - \frac{0.4 \times F_{post} \times e_{uc}}{S_{bc}} \quad \text{(A3)}$$

Here, e_{up} and e_{uc} are the eccentricity of unbonded post-tensioning strands with respect to the centroids of precast and composite sections, respectively. From Table A1, values of e_{up} and e_{uc} are 19.12 and 21.67 in., respectively. Substituting the values in Eq. (A3),
$(\sigma_c)_{b2}$ = –0.938 ksi

The cracking moment (M_{cr}) can be found from the following expression:

$$(\sigma_c)_{b1} + (\sigma_c)_{b2} + M_{cr}/S_{bc} = f_r \quad \text{(A4)}$$

Here, S_{bc} is the section modulus of composite section with

Table A1. Section properties of DT beam cross section.

Sectional properties	Precast section	Composite section
Cross-sectional area, sq in.	1462	1673
Moment of inertia, in.^{4}	328,489	403,821
Distance of centroid of the section from the bottom fiber of the section	29.35	31.90
Distance of centroid of the section from the top fiber of the section	18.68	19.08
Section modulus corresponding to the bottom fiber of section	11,192	12,659
Section modulus corresponding to the top fiber of section	17,585	21,165
Eccentricity of resultant pretensioned force, in.	13	N/A
Eccentricity of unbonded post-tensioning strands, in.	19.12	21.67

Note: 1 in. = 25.4 mm; 1 sq in. = 645 mm^2; 1 in.^{3} = 16387 mm^3; 1 in.^{4} = 416231 mm^4.
N/A refers to a non-applicable value for calculating stresses and/or moment due to pretensioning forces because pretensioning forces were not applied to the composite section.

respect to extreme tension fiber and is equal to 12,659 in.^{3} (see Table A1). Substituting the values in Eq. (A4),

M_{cr} = 3212.2 kip-ft

Thus, cracking load,

$$P_{cr} = \frac{(M_{cr} - M_D) \times 2}{27.5}$$

= 147.2 kips > service load (104.3 kips)

Percent difference between the theoretical and experimental cracking loads:

$$= \frac{(147.2 - 144.7)}{144.7} \times 100$$

= 1.7 percent

Step 4 — Compute flexural moment capacity:

Ultimate bond reduction coefficient for external strands,

$$\Omega_u = \frac{5.4}{\frac{L_u}{d_u}} \quad \text{(A5)}$$

where

L_u = horizontal distance between anchorages of unbonded post-tensioning tendons = 51.4 ft

d_u = distance at midspan of external post-tensioning strands from the extreme compression fiber = 40.75 in.

Substituting the values in Eq. (A5), we get $\Omega_u = 0.36$.

Distance of the centroid of bottom bonded pretensioning tendons from the extreme compression fiber, d_m = 47 in.

Flange width, b = 83.46 in.

Total effective pretensioning force, ΣF_{pi} = 854.5 kips

Total effective post-tensioning force, F_{pui} = 397.8 kips

It should be noted that the actual reinforcement ratio of the section is defined as the ratio of total weighted area of the tendons and/or strands in the section to the effective concrete area. Here, weighting factor is defined as the ratio of the stress in a particular equivalent* tendon/strand to the specified strength of bonded pretensioning tendons. The expression for the reinforcement ratio is based on equilibrium of forces in concrete and tendons and the strain compatibility conditions (see Fig. A1).

Flexural stress in the equivalent bonded prestressing tendon at balanced condition, f_{pbb} = 188.7 ksi

Stress in the equivalent non-prestressing strand of webs at balanced condition, f_{pnbb} = 152.4 ksi

Stress in the equivalent unbonded strand at balanced condition, f_{pub} = 72.2 ksi

Stress in the equivalent non-prestressing tendons of flange at balanced condition, f_{pnf} = 39.94 ksi

Total cross-sectional area of bonded prestressing tendons, A_{pb} = 6.66 sq in.

Total cross-sectional area of non-prestressing strands in the webs, A_{pn} = 3.304 sq in.

Total cross-sectional area of unbonded prestressing strands, A_{fu} = 4.68 sq in.

Total cross-sectional area of non-prestressing tendons in the flange, A_{pnf} = 2.109 sq in.

Reinforcement ratio,

$$\rho = \frac{\sum_{j=1}^{m} F_{pi} + f_{pbb}A_{pb} + f_{pnbb}A_{pn} + F_{pui} + f_{pub}A_{fu} - f_{pnfb}A_{pnf}}{b \times d_m \times f_{fu}} \quad \text{(A6)}$$

$$= \frac{854.5 + 188.7 \times 6.66 + 152.4 \times 3.304 + 397.8 + 72.2 \times 4.68 - 39.94 \times 2.109}{83.46 \times 47 \times 415}$$

= 0.002 > 0.0017 (ρ_b)

Since the section is over-reinforced, failure of the beam will occur due to crushing of the concrete topping. The steps to calculate the moment capacity of the DT beam are given below:

* Equivalent tendon/strand means a tendon/strand located at centroid of tendons/strands and having cross-sectional area equal to the total cross-sectional area of corresponding tendons/strands.

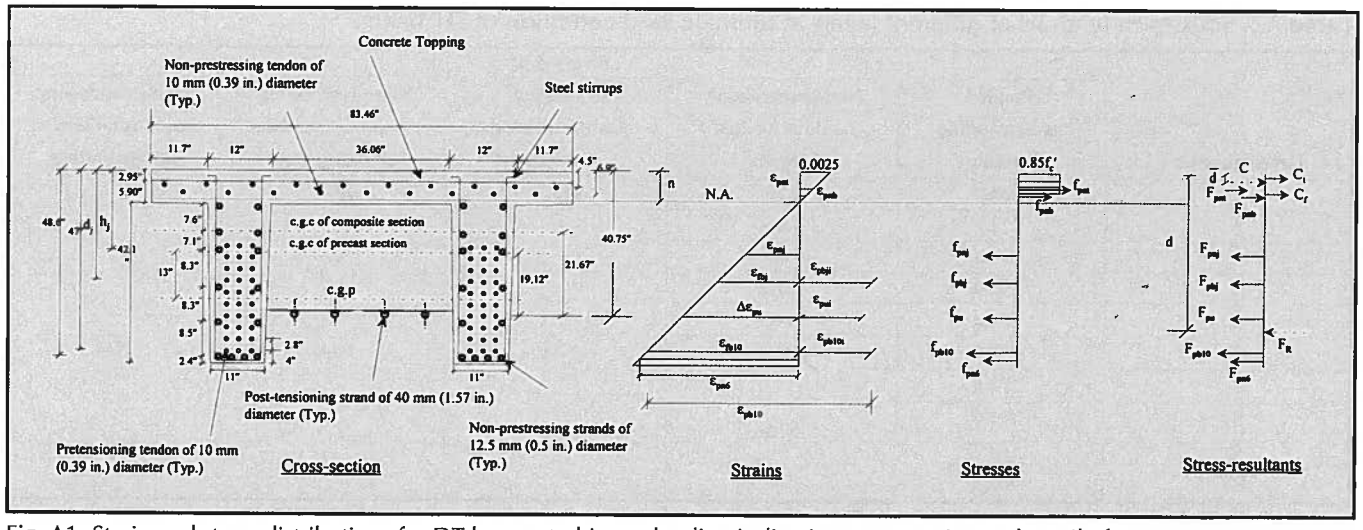

Fig. A1. Strain and stress distributions for DT beam at ultimate loading indicating compressive and tensile forces.

a. Compute strain in tendons/strands:

The strains in tendons/strands can be calculated from the strain distribution as shown in Fig. A1. The ultimate failure of the DT beam was initiated by partial separation between the topping and the beam flange, which led to crushing of the concrete at the strain level of 0.0025. Thus, strain in the concrete at the extreme compression fiber, $\varepsilon_{cu} = 0.0025$.

Let c = depth to the neutral axis from the extreme compression fiber

Strain in bonded prestressing tendons,

$$\varepsilon_{pbj} = \frac{0.0025\times(d_j - c)}{c} + \varepsilon_{pbji} \quad (\text{for } j = 1,\ m) \qquad (A7)$$

Strain in unbonded post-tensioning strands,

$$\varepsilon_{pu} = \frac{0.0025\times(d_u - c)}{c}\Omega_u + 0.0046 \qquad (A8)$$

Strain in non-prestressing strands,

$$\varepsilon_{pnj} = \frac{0.0025\times(h_j - c)}{c} \qquad (A9)$$

Strain in non-prestressing tendons at flange top,

$$\varepsilon_{pnt} = \frac{0.0025\times(c - d_t)}{c} \qquad (A10)$$

Strain in non-prestressing tendons at flange bottom,

$$\varepsilon_{pnb} = \frac{0.0025\times(c - d_b)}{c} \qquad (A11)$$

In Eq. (A7), e_{pbji} equals 0.0059 (for j = 1, 5) and 0.0062 (for j = 6 to 10); d_j (j =1 to 10) is the depth of an individual layer, j, of the bonded pretensioning tendons from the extreme compression fiber. Here, d_1, d_2, d_3, d_4, d_5, d_6, d_7, d_8, d_9, and d_{10} are 21.8, 24.6, 27.4, 30.2, 33.0, 35.8, 38.6, 41.4, 44.2, and 47.0 in., respectively; d_u is the depth of unbonded post-tensioning tendons from the extreme compression fiber and is equal to 40.75 in.

In Eq. (A9), h_j (j = 1 to 6) is the depth of an individual layer, j, of the non-prestressing tendons provided in webs. Here, h_1, h_2, h_3, h_4, h_5, and h_6 are 8.8, 16.4, 23.5, 31.8, 40.1, and 48.6 in., respectively; d_t [see Eq. (A10)] and d_b [see Eq. (A11)] are the depth of the top and bottom layers of non-prestressing tendons provided in the flange, respectively. Here, d_t and d_b are 4.5 and 6.9 in., respectively.

b. Compute resultant forces in tendons/strands and concrete:

Total cross-sectional area of bonded prestressing tendons in each row, A_{fb} = 0.666 sq in.

Total cross-sectional area of non-prestressing strands in each row, A_{fn} = 0.472 sq in. for Rows 1 to 5 and A_{fn} = 0.944 sq in. for Row 6.

Total cross-sectional area of non-prestressing tendons at flange top, A_{fnt} = 1.11 sq in.

Total cross-sectional area of non-prestressing tendons at flange bottom, A_{fnb} = 0.999 sq in.

Using the stress-strain and force-stress relationships (i.e., stress = strain × modulus of elasticity; and force = stress × cross-sectional area of tendons of each layer), the resultant forces in each layer of prestressing and non-prestressing tendons can be determined by the following expressions:

Resultant force in pretensioning tendons,

$$F_{pbj} = \left[\frac{35.5(d_j - c)}{c} + 83.78\right] \text{kips for } j = 1 \text{ to } 5 \qquad (A12a)$$

$$F_{pbj} = \left[\frac{35.5(d_j - c)}{c} + 88.03\right] \text{kips for } j = 6 \text{ to } 10 \qquad (A12b)$$

Resultant force in unbonded post-tensioning strands,

$$F_{pu} = \left[\frac{77.6\ \ (40.75 - c)}{c} + 396.54\right] \text{kips} \qquad (A13)$$

Table A2. Stresses in tendons of different layers at ultimate load condition of DT beam.

Layer number	Stress (ksi)				
	Bonded pretensioning tendons	Non-prestressing tendons located in webs	Unbonded post-tensioning tendons	Non-prestressing tendons located at flange top	Non-prestressing tendons located at flange bottom
1	205.6	0.40	145.5	25.8	11.2
2	222.7	43.6	N/A	N/A	N/A
3	239.8	84.0			
4	256.9	131.2			
5	274.0	178.5			
6	297.5	226.8			
7	314.5	N/A			
8	331.6				
9	348.7				
10	365.8				

Note: 1 ksi = 6.895 MPa.

Resultant force in non-prestressing strands,

$$= \frac{23.45(h_j - c)}{c} \text{ kips} \quad \text{for } j = 1 \text{ to } 5 \qquad \text{(A14a)}$$

$$= \frac{46.9(h_j - c)}{c} \text{ kips} \quad \text{for } j = 6 \qquad \text{(A14b)}$$

Resultant force in non-prestressing tendons at flange top,

$$F_{pnt} = \frac{59.2(c - 4.5)}{c} \text{ kips} \qquad \text{(A15)}$$

Resultant force in non-prestressing tendons at flange bottom,

$$F_{pnb} = \left[\frac{53.3\ (c - 6.9)}{c}\right] \text{ kips} \qquad \text{(A16)}$$

Compressive force in concrete = $C_t + C_f$
$= 0.85f'_c(E_{ct}/E_c)bh_t + 0.85f'_c b(0.66c - 2.95)$
$= [1405.62 + 554.05\ (0.66c - 2.95)]$ kips (A17)

c. Compute the neutral axis depth *c*:

From the equation of equilibrium,

$$\sum_{j=1}^{10} F_{pbj} + \sum_{j=1}^{6} F_{pnj} + F_{pu} = C \qquad \text{(A18)}$$

$$\frac{35.5}{c}(344 - 10c) + 859.05 + \frac{23.45}{c}(217.8 - 7c) + \frac{77.6}{c}(40.75 - c) + 396.54$$
$$= 1405.62 + 554.05(0.66c - 2.95) + \frac{59.2(c - 4.5)}{c} + \frac{53.3(c - 6.9)}{c}$$

Solving for c gives $c = 8.73$ in.

d. Compute stresses in tendons/strands:

The value of strain in tendons/strands can be computed using Eqs. (A7) through (A11), and then using the stress-strain relationships, stresses in tendons/strands of different layers can be calculated.

For example, stress in the tenth layer of bonded pretensioning tendons

$$= \left[\frac{0.0025\ (47 - c)}{c} + 0.0062\right] \times 21{,}320$$
$= 365.8$ ksi $<$ 415 ksi (OK)

The calculated values of the stress in tendons of different layers are presented in Table A2.

e. Compute the resultant force in tendons and concrete:

Resultant forces in tendons of different layers can be calculated by multiplying the corresponding tendons stress and equivalent cross-sectional area of tendons of a particular layer. For example, resultant force in pretensioning tendons of 10th layer is given by:

$F_{pb10} = 365.8 \times 0.666$
$= 243.6$ kips

The calculated resultant forces in tendons of different layers are presented in Table A3.

From Eq. (A17), resultant force in concrete = $C_t + C_t$ = 2963.5 kips

Total compressive force,

$C = C_t + C_f + F_{pnt} + F_{pnb}$
$= 2963.5 + 28.6 + 11.2$
$= 3003.2$ kips

Total resultant tension force,

$$F_R = \sum_{j=1}^{10} F_{pbj} + \sum_{j=1}^{6} F_{pnj} + F_{pu}$$
$= 3004.3$ kips $\cong C$ (OK)

Table A3. Resultant forces in tendons of different layers at ultimate load condition of DT beam.

Layer number	Force (kips)				
	Bonded pretensioning tendons	Non-prestressing tendons located in webs	Unbonded post-tensioning tendons	Non-prestressing tendons located at flange top	Non-prestressing tendons located at flange bottom
1	136.9	0.2	680.9	28.6	11.2
2	148.3	20.6	N/A	N/A	N/A
3	159.7	39.6			
4	171.1	61.9			
5	182.5	84.3			
6	198.1	214.1			
7	209.5	N/A			
8	220.8				
9	232.2				
10	243.6				

Note: 1 kip = 4.44 kN.

f. Compute the ultimate moment capacity:

Location of the center of gravity of the resultant tension force measured from the extreme compression fiber, $d = 37.61$ in.

Depth of Whitney's equivalent stress block,

$a = \beta_1 c$

$= 0.66 \times 8.73$

$= 5.76$ in.

Distance of the center of gravity of resultant compression force from the extreme compression fiber,

$$\bar{d} = \frac{1405.6 \times \frac{2.95}{2} + 1557.9 \times \left(2.95 + \frac{2.81}{2}\right) + 28.3 \times 4.5 + 10.6 \times 6.9}{3003.2}$$

$= 3.02$ in.

Thus, nominal moment capacity,

$M_n = F_R(d - \bar{d})$

$= 3004.3 \times (37.61 - 3.02)$

$= 8659.9$ kip-ft

Design moment capacity,

$M_u = 0.85 \times 8659.9$

$= 8210.9$ kip-ft > 4102.34 kip-ft ($M_{required}$) (OK)

g. Compare the theoretical and experimental values of moment capacity and post-tensioning tendon force:

Experimental value of the moment capacity of DT beam = [(549 × 227.5)/2] + 1188.8 = 8739.0 kip-ft

Theoretical nominal moment capacity of DT beam = 8659.9 kip-ft

Percent difference in experimental and theoretical moment capacities,

$$= \frac{(8739.0 - 8659.9)}{8739.0} \times 100$$

$= 0.9$ percent

Experimental value of post-tensioning force in each post-tensioning strand = 181.3 kips

Theoretical value of post-tensioning force in each tendon = 680.9/4 = 170.2 kips

Percent difference in experimental and theoretical values of post-tensioning force

$$= \frac{(181.3 - 170.2)}{181.3} \times 100$$

$= 6.1$ percent

h. Compute stresses due to service loads:

Moment due to service loads, $M = 1188.8 + 1434.13 = 2622.93$ kip-ft < 3203.9 kip-ft (cracking moment)

Since moment due to service loads is less than the cracking moment, the section will remain uncracked at the service load. The maximum stresses can be calculated as follows:

Maximum compressive stress in concrete at the extreme compression fiber,

$$f_{ct} = \frac{F_{pre}}{A_p} - \frac{F_{pre} e_b}{S_{tp}} + \frac{0.6 \times F_{post}}{A_p} - \frac{0.6 \times F_{post} e_{up}}{S_{tp}} + \frac{0.4 \times F_{post}}{A_c} - \frac{0.4 \times F_{post} \times e_{uc}}{S_{tc}} + \frac{M}{S_{tc}} \quad \text{(A19)}$$

Substituting the values of sectional properties (see Table A1) and other parametric values in Eq. (A19), we get $f_{ct} = 1.28$ ksi < 4.69 ksi ($0.6f'_c$) (OK)

Maximum concrete stress due to applied load

$$= \frac{1434.13 \times 12}{21{,}165}$$

$= 0.81$ ksi

Experimental value of concrete stress = 1.0 ksi

Percent difference in theoretical and experimental values of concrete stress

$$= \frac{1.0 - 0.81}{1.0} \times 100$$

$$= 19 \text{ percent}$$

This difference in analytical and experimental strain in concrete topping may be attributed to the change in the strain condition because of the changing of the support condition of the beam during various construction stages and due to different properties of the concrete topping and precast concrete.

Stress in bottom prestressing tendons,

$$f_{pb10} = E_f \varepsilon_{pb10i} + \frac{E_f}{E_c} \frac{M(d_{10} - y_{tc})}{I_c} \quad \text{(A20)}$$

$$= 21{,}320 \times 0.0062 + 4.0 \times \frac{2622.93 \times 12 \times (47.0 - 19.08)}{40{,}3821}$$

$$= 132.19 + 8.70$$

$$= 140.89 \text{ ksi} < 415 \text{ ksi} \quad \text{(OK)}$$

Stress in bottom prestressing tendons due to applied load

$$= 4.0 \times \frac{1434.13 \times 12 \times (47 - 19.08)}{40{,}3821}$$

$$= 4.76 \text{ ksi} \cong 4.73 \text{ ksi (experimental value)}$$

Stress in post-tensioning strands,

$$f_{pu} = E_{fp} \varepsilon_{pui} + \frac{E_{fp}}{E_c} \frac{(M - M_D) e_{uc}}{I_c} \Omega$$

$$= 18{,}419 \times 0.0046 + 3.46 \times \frac{(2622.93 - 1188.8) \times 12 \times 21.67}{403{,}821} \times \frac{2}{3}$$

$$= 86.86 \text{ ksi} < 271 \text{ ksi} \quad \text{(OK)}$$

Force in a CFCC strand at service load = 86.86 × 1.17 = 101.63 kips

Experimental value of post-tensioning force = 101.12 kips

Percent difference in theoretical and experimental values of post-tensioning force at service load

$$= \frac{101.63 - 101.12}{101.12} \times 100$$

$$= 0.5 \text{ percent}$$

i. Compute maximum deflection under service load (no cracking occurs under service load):

$$M_L = M - M_D$$

$$= 1434.13 \text{ kip-ft}$$

Distance between the support and nearest load point, $L_1 = 27.5$ ft

Longitudinal distance between load points, $L_2 = 12$ ft

Deflection due to applied load,

$$\delta_a = \frac{M_L L_1^2}{8 E_c I_c} \left[\frac{8}{3} + 4.0 \left(\frac{L_2}{L_1} \right) + \left(\frac{L_2}{L_1} \right)^2 \right] \quad \text{(A21)}$$

$$= \frac{1434.13 \times 12 \times (27.5 \times 12)^2}{8 \times 5320 \times 40{,}3821} \left[\frac{8}{3} + 4.0 \left(\frac{12}{27.5} \right) + \left(\frac{12}{27.5} \right)^2 \right]$$

$$= 0.502 \text{ in.} \downarrow \cong 0.505 \text{ in. (experimental value)}$$

It should be noted that the precast DT beam was supported at Diaphragms D2 and D6 prior to initial post-tensioning. The center-to-center distance between Diaphragms D1 and D2, d_{12}, was 7.8 ft. Hence, midspan deflection of DT beam due to dead load is given by

$$\delta_d = \frac{144}{E_c I_p} \left[\frac{W_D L^4}{384} - \frac{W_D L}{12} \left(\frac{L}{2} - d_{12} \right)^3 + 5081.85L - 79603.8 \right] \text{ in.}$$

$$\delta_d = \frac{144}{5320 \times 328{,}489} \left[\frac{2.12 \times 67^4}{384} - \frac{2.12 \times 67}{12} \left(\frac{67}{2} - 7.8 \right)^3 + 5081.85 \times 67 - 79603.8 \right]$$

$$= 0.01 \text{ in.} \downarrow$$

Assuming that the loss of pretensioning forces up to the instant of initial post-tensioning be negligible,

Effective pretensioning force = 1139.3 kips

Deflection due to pretensioning force at the instant of initial post-tensioning

$$= \frac{1139.3 \times 13.0 \times (67 \times 12)^2}{8 \times 5320 \times 328{,}489}$$

$$= 0.69 \text{ in.} \uparrow$$

Center-to-center distance between Diaphragms D2 and D6 = 51.4 ft

Deflection due initial post-tensioning

$$= \frac{0.6 \times 397.8 \times 19.12 \times (51.4 \times 12)^2}{8 \times 5320 \times 32{,}8489}$$

$$= 0.12 \text{ in.} \uparrow$$

Total deflection of the precast DT beam after the initial post-tensioning

$$= 0.69 + 0.12 - 0.01$$

$$= 0.80 \text{ in.} \uparrow$$

Experimental value of deflection due to pretensioning and initial post-tensioning = 0.79 in. ↑

Percent difference in theoretical and experimental values of deflection after initial post-tensioning

$$= \frac{0.80 - 0.79}{0.79}$$

$$= 1.3 \text{ percent}$$

Measured loss in the deflection due to transportation and support condition change = 0.25 in. ↓

Net deflection due to prestressing prior to final post-tensioning

= 0.80 – 0.25

= 0.55 in. ↑

Increase in deflection due to final post-tensioning

$$= \frac{0.4 \times 397.8 \times 21.67 \times (51.4 \times 12)^2}{8 \times 5320 \times 40,3821}$$

= 0.08 in. ↑

Weight of the concrete topping

$$= \frac{150 \times 83.46 \times 2.95}{12^2 \times 1000}$$

= 0.26 kip / ft

Deflection due to concrete topping

$$= \frac{5}{384} \frac{0.26 \times (67 \times 12)^4}{12 \times 5320 \times 403,821}$$

= 0.05 in. ↓

Net deflection at the time of final post-tensioning

= 0.55 + 0.08 – 0.05

= 0.58 in. ↑

Experimental value of the net deflection after final post-tensioning = 0.56 in. ↑

Percent difference in theoretical and experimental values of deflection after final post-tensioning

$$= \frac{0.58 - 0.56}{0.56} \times 100$$

= 3.6 percent

APPENDIX B — NOTATION

a = depth of equivalent rectangular compression block, in.

A_c = cross-sectional area of composite DT beam, sq in.

A_p = cross-sectional area of precast DT beam, sq in.

A_{fb} = cross-sectional area of bottom bonded prestressing tendons in each row, sq in.

A_{fn} = cross-sectional area of non-prestressing tendons in each row, sq in.

A_{fnt} = cross-sectional area of non-prestressing tendons at flange top, sq in.

A_{fnb} = cross-sectional area of non-prestressing tendons at flange bottom, sq in.

A_{fu} = total cross-sectional area of unbonded post-tensioning tendons, sq in.

A_{pb} = total cross-sectional area of bonded prestressing tendons, sq in.

A_{pn} = total cross-sectional area of non-prestressing tendons in the webs, sq in.

A_{pnf} = total cross-sectional area of non-prestressing tendons in the flange, sq in.

b = width of compression face of member, in.

c = depth to the neutral axis from the extreme compression fiber, in.

C = resultant compressive force, kips

C_t = resultant compression force in concrete topping, kips

C_f = resultant compression force in flange of precast DT beam, kips

c.g.c = axis passing through the centroid of concrete cross section of the DT beam

c.g.p = axis passing through the center of gravity of the resultant pretensioned force

d_{12} = center-to-center distance between Diaphragms D1 and D2, ft

d = distance to center of gravity of the resultant tension force from the extreme compression fiber, in.

$\bar{d}$ = distance to center of gravity of the resultant compression force from the extreme compression fiber, in.

d_j = distance to centroid of bonded prestressing tendons of an individual row from the extreme compression fiber, in.

d_m = distance to centroid of bottom bonded prestressing tendons (mth row) from the extreme compression fiber, in.

d_b = distance to centroid of non-prestressing tendons at flange bottom from the extreme compression fiber, in.

d_t = distance to centroid of non-prestressing tendons at flange top from the extreme compression fiber, in.

d_u = distance to centroid of unbonded post-tensioning

tendons from the extreme compression fiber, in.

e_b = eccentricity of resultant pretensioning force from the centroid of the precast concrete cross section, in.

e_{up} = eccentricity of unbonded post-tensioning tendons from centroid of the precast concrete cross section, in.

e_{uc} = eccentricity of unbonded post-tensioning tendons from the centroid of composite section

E_c = modulus of elasticity of precast concrete, ksi

E_{ct} = modulus of elasticity of concrete topping, ksi

E_f = modulus of elasticity of bonded tendon, ksi

E_{fn} = modulus of elasticity of non-prestressing tendons in webs, ksi

E_{fp} = modulus of elasticity of unbonded tendon, ksi

f_c = stress in the concrete at extreme compression fiber in very under-reinforced beam, ksi

f_{ct} = stress in the concrete at extreme compression fiber in over-reinforced beam, ksi

f'_c = specified compressive strength of precast concrete, ksi

f_{fu} = specified ultimate tensile strength of bonded prestressing tendons, ksi

f_{fun} = specified ultimate tensile strength of non-prestressing tendons in webs, ksi

f_{fup} = specified ultimate tensile strength of unbonded post-tensioning tendons, ksi

f_{pbb} = flexural stress in the equivalent bonded prestressing tendons at balanced condition, ksi

f_{pbj} = total stress in bonded prestressing tendons of an individual row, ksi

f_{pbm} = total stress in bottom prestressing tendons (mth row), ksi

f_{pbmi} = initial effective prestress in bottom bonded prestressing tendons (mth row), ksi

f_{pnb} = total stress in non-prestressing tendons at flange bottom, ksi

f_{pnbb} = stress in the equivalent non-prestressing tendon in the webs, ksi

f_{pnfb} = stress in the equivalent non-prestressing tendon in the flange, ksi

f_{pnj} = total stress in non-prestressing tendons of an individual row in webs, ksi

f_{pnk} = total stress in non-prestressing tendons of bottom row (kth row), ksi

f_{pnt} = total stress in non-prestressing tendons at flange top, ksi

f_{pu} = total stress in unbonded post-tensioning tendons, ksi

f_r = modulus of rupture of concrete, psi

F_{pi} = initial effective prestress in bonded pretensioning tendons, kips

F_{pre} = resultant effective pretensioning force in bonded tendons, kips

F_{post} = resultant effective post-tensioning force in unbonded tendons, kips

F_{pbj} = resultant tensile force in bonded prestressing tendons of an individual row, kips

F_{pbm} = resultant tensile force in bonded bottom (mth row) prestressing tendons, kips

F_{pnb} = resultant compression force in non-prestressing tendons at flange bottom, kips

F_{pnj} = resultant tensile force in non-prestressing tendons of individual row in webs, kips

F_{pnk} = resultant tensile force in non-prestressing tendons of bottom row (kth row) in webs, kips

F_{pnt} = resultant compression force in non-prestressing tendons at flange top, kips

F_{pu} = resultant tensile force in unbonded post-tensioning tendons, kips

F_{pui} = total initial effective post-tensioning force, kips

F_R = resultant of the tensile forces in bonded and unbonded tendons, kips

h_f = flange thickness of DT beam, in.

h_j = distance of centroid of non-prestressing tendons of an individual row in webs, in.

h_k = distance of centroid of bottom non-prestressing tendons (kth row), in.

h_t = thickness of concrete topping, in.

I_c = moment of inertia of composite concrete cross section, in.^{4}

I_p = moment of inertia of precast concrete cross section, in.^{4}

k = number of rows of non-prestressing tendons in webs of DT beam

L = effective span of the beam, ft

L_u = horizontal distance between the ends of unbonded post-tensioning strand, ft

m = number of rows of bonded tendons

M = applied maximum moment due to service loads, kip-ft

M_{cr} = cracking moment capacity of section, kip-ft

M_u = design moment capacity of section, kip-ft

M_D = maximum bending moment due to dead load, kip-ft

M_L = maximum bending moment due to live load, kip-ft

M_n = nominal moment capacity of section, kip-ft

$M_{required}$ = required moment capacity of the section, kip-ft

p = number of materials used for tension reinforcement

P_{cr} = midspan load causing cracking of DT beam, kips

S_{bc} = section modulus corresponding to the bottom extreme fiber of composite section, in.^{3}

S_{bp} = section modulus corresponding to the bottom extreme fiber of precast section, in.^{3}

S_{tp} = section modulus corresponding to the top extreme fiber of precast section, in.^{3}

S_{tc} = section modulus corresponding to the top extreme fiber of composite section, in.^{3}

W = total midspan load, kips

W_d = self-weight of beam per unit length, kip/ft

$\bar{y}$ = distance of centroid of tension reinforcement from the extreme compression fiber, in.

y_{bc} = distance of centroid of composite section from the bottom fiber, in.

y_{bp} = distance of centroid of precast section from the bottom fiber, in.

y_{tc} = distance of centroid of composite cross section from the top fiber, in.

β_1 = factor defined as the ratio of the equivalent rectangular stress block depth to the distance from the extreme compression fiber to the neutral axis

ε_{cu} = ultimate compression strain in concrete (0.0025)

ε_{fbj} = flexural strain in the bonded prestressing tendons of an individual row

ε_{fbm} = flexural strain in the bonded prestressing tendons of bottom row (mth row)

ε_{fu} = ultimate tensile strain capacity of bonded prestressing tendons

ε_{fun} = ultimate tensile strain capacity of non-prestressing tendons in webs

ε_{fup} = ultimate tensile strain capacity of unbonded tendons

ε_{pbj} = total strain in bonded prestressing tendons of an individual row

ε_{pbji} = initial strain in bonded prestressing tendons of an individual row

ε_{pbm} = total strain in bonded prestressing tendons of mth row

ε_{pbmi} = initial strain in bonded prestressing tendons of mth row

ε_{pnb} = total strain in non-prestressing tendons at flange bottom

ε_{pnj} = total strain in non-prestressing tendons of an individual row in webs

ε_{pnk} = total strain in non-prestressing tendons of bottom row (kth row)

ε_{pnt} = total strain in non-prestressing tendons at flange top

ε_{pu} = total strain in unbonded post-tensioning tendons

ε_{pui} = initial strain in unbonded post-tensioning tendons

$\Delta\varepsilon_{pu}$ = flexural strain in unbonded post-tensioning tendons

α = ratio of the effective post-tensioning force applied to the precast DT beam to the total effective post-tensioning force

$(\sigma_c)_{b1}$ = stress at extreme tension fiber due to pretensioning force, ksi

$(\sigma_c)_{b2}$ = stress at extreme tension fiber due to post-tensioning force, ksi

ρ = tensile reinforcement ratio

ρ_b = balanced ratio

Ω_u = bond reduction coefficient at ultimate

δ = maximum midspan deflection of the beam under service loads, in.

δ_a = maximum midspan deflection of the beam due to applied load, in.

δ_d = maximum midspan deflection of the beam due to dead load, in.

δ_p = maximum midspan deflection of the beam due to prestressing forces, in.